ARTICLE

Strong Hierarchically Porous Monoliths by Pulsed Current Processing of Zeolite Powder Assemblies

Petr Vasiliev,[†,§] Farid Akhtar,[†] Jekabs Grins,[†] Johanne Mouzon,[‡] Charlotte Andersson,[‡] Jonas Hedlund,[‡] and Lennart Bergström*[,†]

Department of Materials and Environmental Chemistry, Arrhenius Laboratory, Stockholm University, Stockholm SE-106 91, Sweden, Department of Applied Chemistry and Geosciences, Division of Chemical Engineering, Luleå University of Technology, Luleå SE-971 87, Sweden, and The Berzelii centre Exselent on porous materials, Stockholm, Sweden

ABSTRACT Binderless hierarchically porous monoliths have been produced from silicalite-1 and ZSM-5 zeolite powders by a rapid and facile powder processing method where the zeolite powders are assembled in a graphite die and subjected simultaneously to a compressive pressure and a pulsed current. Pulsed current processing (PCP) or, as it is commonly called, spark plasma sintering, enables rapid thermal processing of zeolite powder assemblies with heating and cooling rates at 100 °C/minute or more, which results in the formation of strong powder bodies without any addition of secondary binders. Nitrogen adsorption measurements show that it is possible to form strong zeolite monoliths by PCP that maintain between 85 and 95 % of the surface area of the as-received silicalite-1 and ZSM-5 powders. Line-broadening analysis of X-ray powder diffraction data by the Rietveld method and high-resolution electron microscopy showed that the formation of strong interparticle bonds is associated with a local amorphization reaction at the interfacial contact points between the zeolite particles. The PCP-treated binderless ZSM-5 monoliths display a high selectivity in xylene isomer separation.

KEYWORDS: zeolite • thermal treatment • spark plasma sintering • porous • catalysis

INTRODUCTION

The well-defined pore size and pore structure of zeolites together with the flexible acid/base surface properties makes them highly useful in a number of industrial applications, e.g., as ion exchangers for water softening, as drying agents or absorbents for organic vapors, as molecular sieves and separation membranes, or as catalyst for the production of petrochemicals (1, 2). The use of zeolites in industrially important applications, e.g., gasoline upgrading and gas purification requires that the primary micrometer-sized zeolite particles are assembled into strong macroscopic secondary structures, i.e., granules, pellets, cylinders, and discs (3−5). Indeed, the preparation of hierarchically porous materials that display a multimodal porosity is a necessary step toward creating porous materials with a high surface area and a low pressure drop for various potential applications in catalysis and adsorption and as support materials.

The current technology for producing, e.g., zeolite monoliths for catalytic and adsorbent applications involves extrusion or pressing zeolite particles together with a nonzeolitic binder, followed by a drying and heating step (4). The nonzeolitic binders are usually added to impart a high mechanical strength and sufficient resistance to attrition. Examples of suitable inorganic binders include alumina, silica, and various types of clays (6).

Fugitive templates, e.g., carbon aerogels (7), polyurethane foams (8), and resin beds (9) have been used to produce hierarchically porous zeolite materials directly during synthesis. It is also possible to deposit zeolite films onto the surfaces of macroporous ceramic foams or honeycomb structures (10−15).

Hydrothermal transformation routes (16, 17) can be used to reduce the amount of nonzeolitic material; zeolite beta monoliths were, e.g., produced via the transformation of the amorphous walls of silica monolith using carbon as a transitional template (18). However, the applicability of the hydrothermal conversion and templating approaches are limited by the lengthy reaction times and elaborate process schemes.

In this study, we show how a rapid and facile powder processing technique, pulsed current processing (PCP), can be used to produce strong hierarchically porous zeolite monoliths from silicalite-1 and ZSM-5 powders without the use of any secondary binders. Line-broadening analysis of X-ray powder diffraction data by the Rietveld method and high-resolution electron microscopy were used to analyze the origin of the formation of strong interparticle bonds during the PCP process. Nitrogen sorption, mercury intrusion, scanning electron microscopy, and diametral compres-

* Corresponding author. E-mail: lennart.bergstrom@mmk.su.se. Tel.: +46 8 16 23 68. Fax: +46 8 15 21 87.
Received for review November 4, 2009 and accepted February 1, 2010
[†] Stockholm University.
[‡] Luleå University of Technology.
[§] The Berzelii centre Exselent on porous materials.
DOI: 10.1021/am900760w
© 2010 American Chemical Society

Published on Web 02/10/2010

sion tests were used to determine the effect of processing temperature on the porosity and mechanical strength of the zeolite secondary structures. The catalytic activity of binderless ZSM-5 monoliths was evaluated by a xylene isomerization study.

EXPERIMENTAL SECTION

Materials. ZSM-5 and silicalite-1 are microporous, crystalline inorganic materials that belong to the MFI type of molecular sieves (19, 20). The ZSM-5 powder with a SiO_2/Al_2O_3 ratio of 280 was obtained from Zeolyst. The silicalite-1 powder was synthesized by first adding 5.29 g of a solution of tetrapropylammonium (TPAOH: 40 wt % solution, Applichemie) and then 7.81 g of precipitated silica (Merck) to 20.25 g of distilled water until a homogeneous gel was formed (21). The mixture was subsequently transferred to a Teflon-lined autoclave and hydrothermal treatment was carried out at 170 °C under autogenous pressure for 24 h. The obtained particles were purified by repeated filtration (Munktell 00H filter paper) and washed with distilled water. After drying the resulting cake at 110 °C for 12 h, the powder was gently disagglomerated in a mortar and calcined for template removal in a tubular furnace at 500 °C for 8 h (heating rate 1 °C/min, cooling rate 1.5 °C/min) under flowing oxygen (100 mL/min). The resulting powder was confirmed to be silicalite-1 by X-ray diffraction (XRD) and consisted mostly of twinned crystals of about $10 \times 10 \times 14\ \mu m^3$ with a narrow size distribution.

The zeolite powders were loaded in cylindrical graphite dies (diameter 12 mm) and treated in vacuum with a uniaxial pressure of 20 MPa at a heating rate of about 100 °C/min using a pulsed current processing apparatus (Dr. Sinter 2050, Sumitomo Coal Mining Co. Ltd., Japan) at maximum temperatures, T_{PCP}, between 900 and 1200 °C where the temperature was held for 3 min before the materials were rapidly cooled down.

Methods. The scanning electron microscope (SEM) JEOL JSM-7000F was used to study both zeolite powders that were thinly spread onto a carbon film supported on a brass stud and zeolite monoliths that were fractured and/or polished. Representative cross sections were obtained using a JEOL SM-09010 cross section polisher operated at 6 kV for 7 h.

X-ray powder diffraction patterns of the as-received zeolite powders and ground PCP-treated monoliths were recorded using $CuK_{\alpha 1}$ radiation and a PANalytical X'pert PRO MPD diffractometer equipped with a Pixel detector.

Nitrogen sorption data were recorded using a Micromeritics ASAP 2020 analyzer. The PCP-treated cylindrical samples and as-received powder were degassed at 573 K and adsorption and desorption data were collected at 77 K. The specific surface areas were calculated using the Brunauer−Emmett−Teller (BET) model in the relative pressure region of 0.05−0.15 p/p_o. The macropore volume and the pore size distribution between 3 nm and 360 μm were determined using mercury intrusion porosimetry (Micromeritics AutoPore III 9410). The surface tension and the contact angle of mercury were set to 485 mN/m and 130°, respectively.

Diametral compression tests were carried out at ambient conditions using an electromechanical testing machine (Zwick Z050, Germany) at a constant cross-head displacement rate of 0.5 mm/min. The test specimens were subjected to a compressive stress using two parallel plates. Tensile strength was calculated as $\sigma_T = 2P/d \cdot t \cdot \pi$, where P = load at failure (N), d = specimen diameter (mm), and t = specimen thickness (mm).

A tubular stainless steel reactor was used for the catalysis experiments. The internal diameter and length of the reactor were 17 mm and 200 mm, respectively. The zeolite materials were mixed with 90 wt % acid leached sea sand and ethanol. The lower portion of the reactor was first loaded with (inert) glass beads and the zeolite/sand mixture was subsequently loaded in the middle of the reactor. Finally, the upper portion of the reactor was filled with glass beads. Glass wool was used as a barrier to stabilize the zeolite/sand mixture and the glass beads in the reactor. The zeolite pellets were ground for 5 min in an automatic mortar grinder (Fritsch Pulverisette 2). The as-received ZSM-5 powders and ground monoliths were heated in a furnace at 500 °C for 6 h, with a heating and cooling rate of 0.2 °C/min to obtain the material in catalytically active H^+ form. The samples were calcined in situ at 450 °C for 6 h prior and in between testing. The feed and the products were analyzed with a gas chromatograph (Varian CP 3800) with a polar column (CP Xylene) and a flame ionization detector (FID) connected online. The product distribution (molar ratio of *m*-xylene/*o*-xylene) was measured three times for each *p*-xylene feed, and the standard deviations ranged from 1 to 3%.

RESULTS AND DISCUSSION

Pulsed current processing (PCP) or, as it is usually called, spark plasma sintering, is a novel powder processing method that has mainly been used to produce dense ceramic materials (22, 23). The PCP method simultaneously subjects powder bodies to a pulsed electrical current and a compressive stress. The electric current generates Joule heat which creates a rapid temperature increase. The rapid heating rates suppress grain growth and allows a fine-grained microstructure to be maintained when consolidating and sintering nanomaterials (23, 24). Recently, we showed that monoliths with a bimodal meso/macro porosity can be produced by the PCP technique from an assembly of mesoporous particles with amorphous silica walls, providing that the maximum temperature (T_{PCP}) is kept sufficiently low to inhibit pore collapse (25). The PCP technique has also been used to produce macro/macroporous monoliths from assemblies of diatomite powders (26).

The as-prepared silicalite-1 particles have a narrow particle size distribution and a well-defined, faceted morphology (Figure 1a). Figure 1b shows that treating the silicalite-1 particles by the pulsed current processing technique at a compressive pressure of 20 MPa and a T_{PCP} of 1100 °C results in the formation of a powder body where the faceted morphology of the individual primary silicalite-1 particles is preserved. Increasing T_{PCP} to 1300 °C results in a collapse of the material and a significant loss of the characteristic features of the primary silicalite-1 particles (Figure 1c). This is corroborated by X-ray powder diffraction studies, which show that a PCP-treatment at T_{PCP} of 1200 °C and above results in a significant loss of crystallinity and a subsequent transformation of the silicalite-1 zeolite to α-cristobalite (Supporting Information, Figure S2). The high magnification scanning electron microscopy image in Figure 1d shows that the faceted silicalite-1 primary particles, PCP-treated at 20 MPa and 1100 °C, deform or even collapse locally at the contact points (shown by the white ovals). More examples are given in the Supporting Information (Figure S3). It is important to note the absence of any necks, i.e., material that has been transported to the grain boundaries, suggests that sintering is insignificant under these conditions. Figure 1e gives examples of various shapes of zeolite monoliths that have been produced using different types of dies.

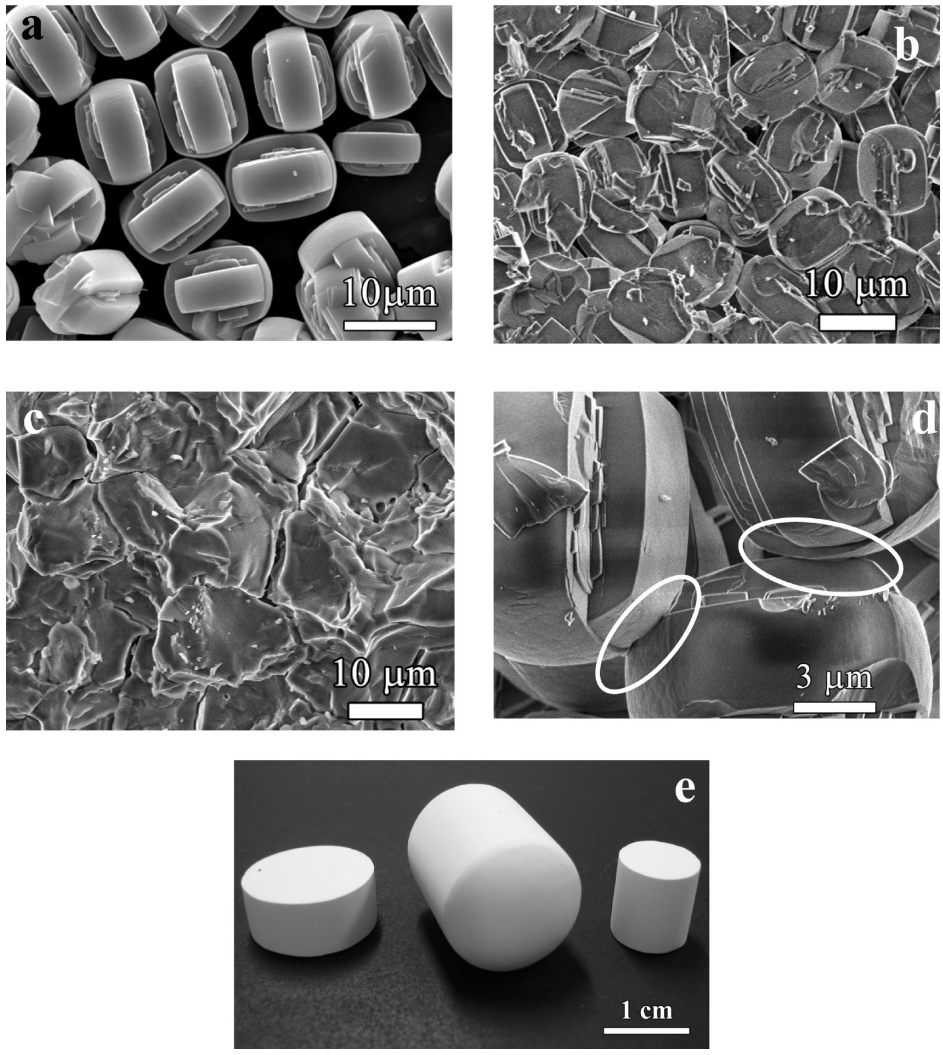

FIGURE 1. Morphology and microstructure of silicalite-1 powders and PCP-treated monoliths. Scanning electron microscopy (SEM) images of (a) as-received silicalite-1 powder; and fracture surfaces of silicalite-1 monoliths prepared at (b) 1100 °C and (c) 1300 °C; and (d) image of higher resolution of silicalite-1 particles PCP-treated at 1100 °C with the partially collapsed contact region indicated by the white ovals. (e) Examples of monoliths produced using different dies.

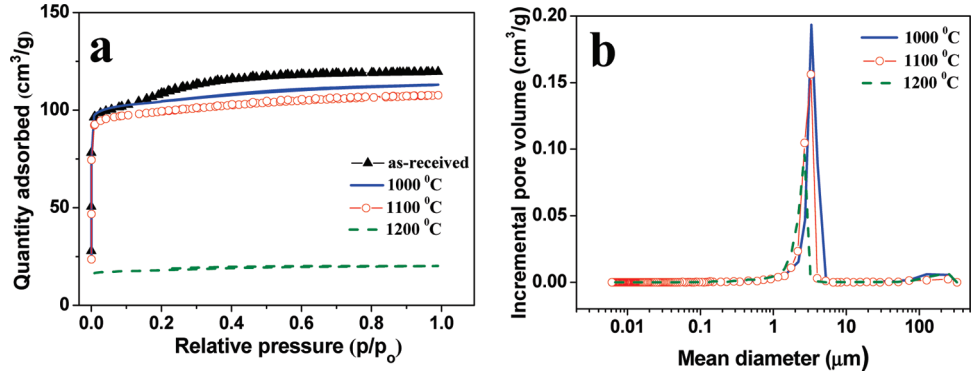

FIGURE 2. Characterization of the porosity of the as-received silicalite-1 powders and monoliths PCP-treated at different temperatures by (a) nitrogen adsorption isotherms and (b) mercury intrusion porosimetry.

Analysis of the nitrogen adsorption isotherms (Figure 2a) shows that PCP-treatment at a T_{PCP} of 1000 and 1100 °C only results in a loss of 3 and 8% of the surface area, respectively, (Table 1) compared to the as-received silicalite-1 powder. At a T_{PCP} of 1200 °C, the BET surface area falls sharply, which suggests that the microporous structure of the zeolite powders have collapsed. Figure 2b shows that the PCP-treated monoliths possess macropores with a size of around 3 μm. This demonstrates that monoliths with well-defined bimodal macro/micro porosity can be produced by PCP-treatment of zeolite powder assemblies. The total volume of the macropores, determined by mercury porosim-

Table 1. Properties of PCP-Treated Monoliths and Powders of Silicalite-1

maximum temperature (T_{PCP}) [°C]	surface area[a] [m^2/g]	total pore volume[b] [cm^3/g]	macropore volume[c] [cm^3/g]	porosity [vol %]	median macropore size [μm]
	376	0.19			
1000	363	0.17	0.39	43	3.3
1100	345	0.17	0.32	37	3.3
1200	62	0.03	0.22	31	2.7

[a] BET surface area calculated within the relative pressure range: 0.05−0.15 p/p_o. [b] Single point adsorption total pore volume at a relative pressure of $p/p_o = 0.99$. [c] Macropore volume calculated by mercury intrusion porosimetry.

Table 2. Properties of PCP-Treated Monoliths and Powders of ZSM-5

maximum temperature (T_{PCP}) [°C]	surface area[a] [m^2/g]	total pore volume[b] [cm^3/g]	macropore volume[c] [cm^3/g]	tensile strength[d] [MPa]
	385	0.21		
950	351	0.21	0.47	0.7
1100	333	0.20	0.44	1.6
1200	304	0.19		2.4
1300	2.5	0.0045		

[a] BET surface area calculated within the relative pressure range: 0.05−0.15 p/p_o. [b] Single point adsorption total pore volume at a relative pressure of $p/p_o = 0.99$. [c] Macropore volume calculated by mercury intrusion porosimetry. [d] Tensile strength obtained from diametral compression of cylindrical pellets.

etry (Table 1), for the silicalite-1 monoliths is relatively large and decrease with increasing T_{PCP}, from 43 vol % at a T_{PCP} of 1000 °C to 31 vol % at a T_{PCP} of 1200 °C.

We have used the PCP-technique to prepare hierarchically porous monoliths also from ZSM-5, which is one of the most industrially important zeolite catalysts (2). Figure 3a shows a fracture surface of a monolith produced from an irregular and highly polydisperse ZSM-5 powder PCP-treated at 20 MPa and a T_{PCP} of 1200 °C. The cross polished section in Figure 3b shows that the primary particles are connected in a network. Similar to the silicalite-1 material, we find that PCP-treatment at 20 MPa up to a T_{PCP} of 1200 °C has a negligible effect on the shape of the nitrogen isotherms (Figure 3c). Analysis of the isotherms verifies (Table 2) that the ZSM-5 monoliths preserve a relatively high surface area and micropore volume up to a T_{PCP} of 1200 °C. However, increasing the T_{PCP} to 1300 °C results in almost total loss of porosity, which can be related to a collapse of both the microporous and macroporous structure of the PCP-treated ZSM-5 monolith. The mercury intrusion data in Figure 3d shows that the ZSM-5 monoliths display a macroscopic pore size around 200−700 nm, which corresponds to the size of the larger interstices between the primary particles and an additional mesoporosity with a pore size around 5−20 nm.

The XRD-data in Figure 4a gives more information on how the PCP treatment influences the structural characteristics of the zeolites. Analysis of the broadening of the X-ray powder diffraction peaks (27, 28) by the Rietveld method and the program FullProf (29) confirmed that the crystallite size is unaffected by the PCP-treatment, which corroborates that any sintering mechanism involving grain growth is of minor importance. Figure 4b shows that the PCP-treatment induces a lattice strain in the zeolite grains, which increases from 0.05% in the as-received material up to 0.17% after PCP-treatment at a temperature of 1150 °C.

We have evaluated the mechanical stability of the ZSM-5 pellets, using the diametral compression test on cylindrical

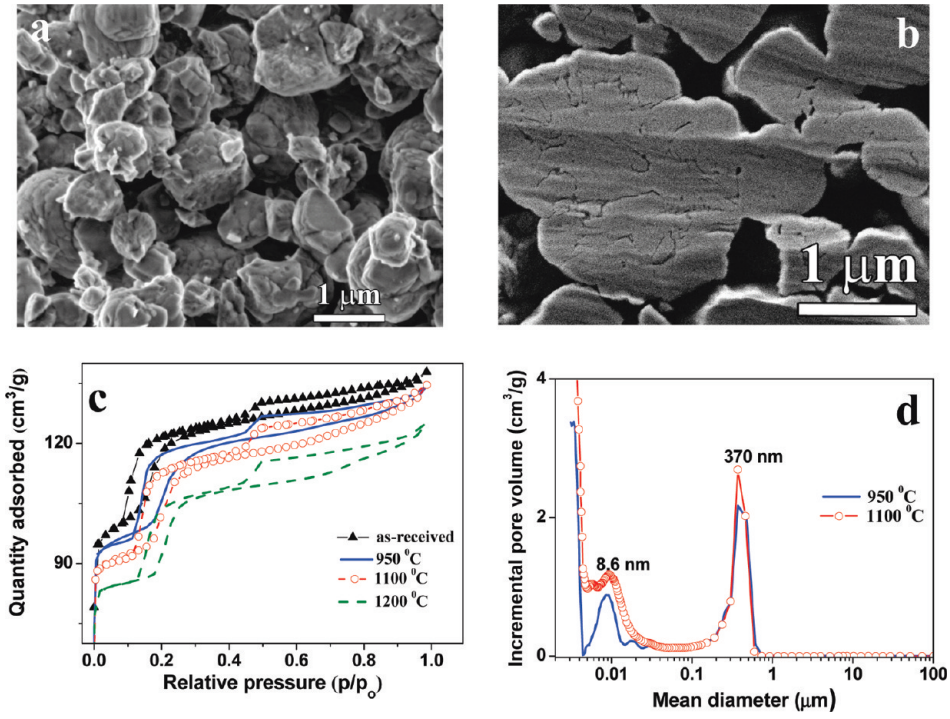

FIGURE 3. Microstructure and porosity of ZSM-5 powders and PCP-treated monoliths. Scanning electron microscopy images: (a) cross section polished and (b) fracture surface of ZSM-5 monoliths prepared at 1200 °C. Characterization of the porosity by (c) nitrogen adsorption isotherms and (d) mercury intrusion porosimetry.

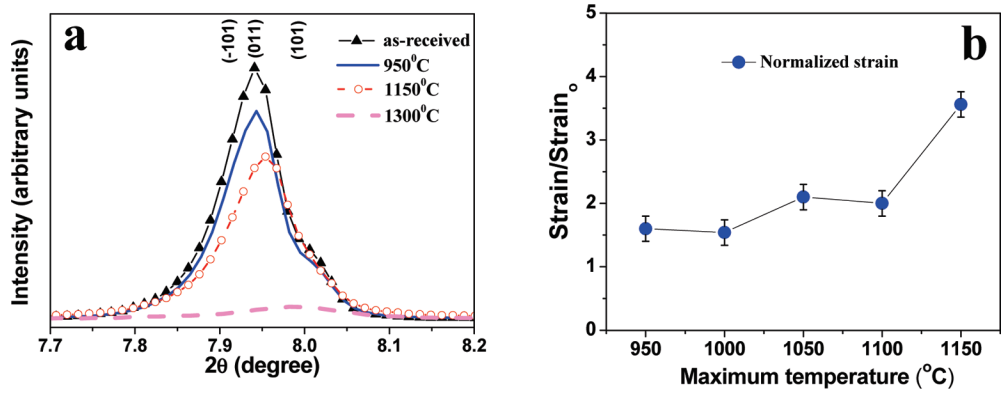

FIGURE 4. Structural properties of ZSM-5 powders and PCP-treated monoliths. Temperature-dependent structural changes probed by (a) the intensity dependence of the compound (−101)/(011) and (101) Bragg reflections of monoclinic ZSM-5; and (b) the estimated normalized normalized lattice strain (Strain/Strain$_o$).

pellets prepared at different T_{PCP}. This simple test subjects a circular disk to a compressive stress between two diametrically opposed plates, and the strength of the material can be related to the tensile stress that develops perpendicularly to the loading direction. Similar to our previous study on PCP-treated mesoporous materials (25), we find that the tensile strength (Table 2) of the zeolite monoliths depends strongly on T_{PCP}. Increasing T_{PCP} from 950 to 1100 °C increases the strength almost three times, from 0.66 to 1.6 MPa, with only a slight decrease of the specific surface area. Increasing T_{PCP} up to 1200 °C increases the strength substantially, to 2.4 MPa, while the specific surface area is still retained above 300 m^2/g. The strength of the binderless zeolite monoliths produced by the PCP-treatment is comparable to the strength of monoliths produced by traditional techniques using substantial amounts of nonzeolitic binders (4) and is substantially higher compared to monoliths produced by other binder-free routes (30).

The significant strength of the monoliths suggests that strong interparticle bonds are formed by the PCP treatment of the zeolite primary particles. The electron microscopy image in Figure 1d indicates that the bond formation is associated with a local collapse of the zeolite grains in contact. Recent experimental (31, 32) and simulation work (33) have shown that zeolites may collapse into amorphous phases of a significantly higher density on heating and/or pressurization. This amorphization process is associated with rearrangement and breakage of bonds, which can promote the formation of new strong bonds between surfaces in close proximity.

Xylene isomerization was used as a probe reaction to evaluate the catalytic activity of the PCP-treated ZSM-5 material. This reaction is well-known and useful to evaluate shape selectivity of acidic zeolite catalysts (34). The equilibrium composition of xylene isomers is about 50% *m*-xylene, 25% *o*-xylene, and 25% *p*-xylene. For *p*-xylene isomerization, the equilibrium conversion is, thus, 75% and the product distribution, i.e., the *m*-/*o*-xylene ratio, will approach 2. At lower conversion, the *m*-/*o*-xylene ratio may be much greater than 2, since *m*-xylene forms first in the series reaction *p*-xylene ↔ *m*-xylene ↔ *o*-xylene (35).

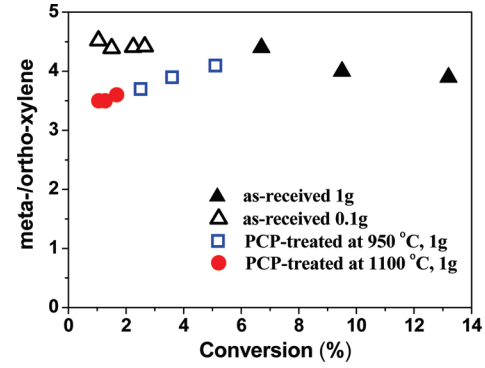

FIGURE 5. Product distribution (molar ratio of *m*-xylene/*o*-xylene) as a function of *p*-xylene conversion for the as-received ZSM-5 powder and the PCP-treated powder at a T_{PCP} of 950 and 1100 °C. The conversion was varied by varying the feed flow rate and the mass of catalyst in the reactor. For a catalyst mass of 1 and 0.2 g, the observed *p*-xylene conversion varied between about 7−13% and 1−3%, respectively, for the as-received ZSM-5 powder.

Figure 5 shows the *m*-/*o*-xylene ratio as a function of conversion for selected ZSM-5 samples. When the reactor was loaded with 0.2 g of the as-received ZSM-powder, an *m*-xylene/*o*-xylene ratio of about 4.4 was observed for a *p*-xylene conversion of about 1−3%. At comparable *p*-xylene conversion, the PCP-treated powders display 10−20% lower *m*-xylene/*o*-xylene ratios (3.5−4.1) compared to the as-received ZSM-5 powder. This is comparable to the decrease of between 5 and 15% of the microporous surface area of the ZSM-5 powders by the PCP-treatment, which could suggest that the performance is directly linked to the available surface area. However, it is difficult to directly compare the xylene isomerization performance of the as-received ZSM-powder and the crushed PCP-treated materials because the PCP-treatment results in a partially amorphized material that can display some additional mass transfer limitations. Unfortunately, it is not possible to prepare a calcined reference ZSM-5 as the microporous material cannot sustain an extended heat treatment at elevated temperatures (950 or 1100 °C).

Also, the PCP-treatment results in a hard material that is difficult to disintegrate by low energy milling; hence, the granule/aggregate size of the PCP-treated material is larger than the as-received powder which also could result in an increased diffusion path. The main products in the *p*-xylene

isomerization test reaction were *o*- and *m*-xylene. However, a slightly larger amount of byproduct (disproportionation products) was obtained (Supporting Information, Figure S5) for the PCP-treated materials at comparable *p*-xylene conversion, which may be related to local heating due to slower transport of the exothermic reaction heat of the larger PCP-treated granules.

CONCLUSIONS

We have shown how mechanically stable, hierarchically porous ZSM-5 and silicalite-1 zeolite pellets can be fabricated by a pulsed current processing technique. Restricting the maximum temperature, T_{PCP}, to below 1200 °C for ZSM-5 and 1100 °C for silicalite-1 results in monoliths with a multimodal macro-, meso-, and microporosity, where at least 85% of the surface area of the as-received microporous zeolites are maintained. Rietveld refinements of X-ray diffraction data and high-resolution electron microscopy suggest that the formation of strong interparticle bonds during the PCP process is associated to a local amorphization reaction at the contact points between the zeolite particles. Xylene isomerization studies showed that the selectivity of the PCP-treated ZSM-5 materials is maintained at a level between 80 and 90% of the as-received ZSM-5 powder. The small differences were related to the minor loss of microporous surface area and a possibly increased mass and heat transfer resistance induced by the PCP-treatment. In summary, the possibility to produce strong, binder-free hierarchically porous zeolite monoliths of an arbitrary shape opens up for new catalysis and adsorption applications where mechanochemical conditions are very demanding.

Acknowledgment. This work was performed within the Berzelii centre Exselent on porous materials. Support from the Swedish Institute for F.A. and the Wallenberg foundation are also gratefully acknowledged. We thank Prof. Zhijian Shen, Prof. Mats Nygren, Dr. Kjell Jansson, Doc. Niklas Hedin, Dr. Robert P. Hodgkins, Mr. Arto Ojuva, and Dr. Wang Lianjun for their advice and assistance during this work. Supporting Information is available online from Wiley InterScience or from the author.

Supporting Information Available: Information on PCP process monitoring, X-ray diffraction and Rietveld analysis, nitrogen sorption isotherms, SEM of silicalite-1 particles in contact, and xylene isomerization; figures displaying uniaxial displacement rates, X-ray diffraction patterns, SEM micrographs, and xylene isomerization. This material is available free of charge via the Internet at http://pubs.acs.org.

REFERENCES AND NOTES

(1) Breck, D. W. In *Zeolite molecular sieves: structure, chemistry, and use*; John Wiley & Sons Inc: New York, 1984.
(2) Weitkamp, J.; Puppe, L. In *Catalysis and zeolites: fundamentals and applications*; Springer-Verlag: Berlin and Heidelberg, 1999.
(3) Crittenden, B.; Thomas, W. J. In *Adsorption technology and design*, Elsevier: New York, 1998.
(4) Satterfield, C. N. In *Heterogeneous catalysis in industrial practice*, Krieger Publishing Company: New York, 1996.
(5) Sherman, J. D. *Proc. Natl. Acad. Sci. U.S.A.* **1999**, *96*, 3471–3478.
(6) Li, Y. Y.; Perera, S. P.; Crittenden, B. D.; Bridgwater, J. *Powder Technol.* **2001**, *116*, 85–96.
(7) Tao, Y. S.; Kanoh, H.; Kaneko, K. *J. Am. Chem. Soc.* **2003**, *125*, 6044–6045.
(8) Lee, Y. J.; Lee, J. S.; Park, Y. S.; Yoon, K. B. *Adv. Mater.* **2001**, *13*, 1259–1263.
(9) Naydenov, V.; Tosheva, L.; Sterte, J. *Chem. Mater.* **2002**, *14*, 4881–4885.
(10) Silva, E. R.; Silva, J. M.; Vaz, M. F.; Oliveira, F. A. C.; Ribeiro, F. *Mater. Lett.* **2009**, *63*, 572–574.
(11) Scheffler, F.; Zampieri, A.; Schwieger, W.; Zeschky, J.; Scheffler, M.; Greil, P. *Adv. Appl. Ceram.* **2005**, *104*, 43–48.
(12) Zampieri, A.; Colombo, P.; Mabande, G. T. P.; Selvam, T.; Schwieger, W.; Scheffler, F. *Adv. Mater.* **2004**, *16*, 819–823.
(13) Sterte, J.; Hedlund, J.; Creaser, D.; Ohrman, O.; Zheng, W.; Lassinantti, M.; Li, Q. H.; Jareman, F. *Catal. Today* **2001**, *69*, 323–329.
(14) Buciuman, F. C.; Kraushaar-Czarnetzki, B. *Catal. Today* **2001**, *69*, 337–342.
(15) Seijger, G. B. F.; Oudshoorn, O. L.; van Kooten, W. E. J.; Jansen, J. C.; van Bekkum, H.; van den Bleek, C. M.; Calis, H. P. A. *Microporous Mesoporous Mater.* **2000**, *39*, 195–204.
(16) Dong, A. A.; Wang, Y. J.; Tang, Y.; Zhang, Y. H.; Ren, N.; Gao, Z. *Adv. Mater.* **2002**, *14*, 1506–1510.
(17) Rauscher, M.; Selvam, T.; Schwieger, W.; Freude, D. *Microporous Mesoporous Mater.* **2004**, *75*, 195–202.
(18) Tong, Y. C.; Zhao, T. B.; Li, F. Y.; Wang, Y. *Chem. Mater.* **2006**, *18*, 4218–4220.
(19) Flanigen, E. M.; Bennett, J. M.; Grose, R. W.; Cohen, J. P.; Patton, R. L.; Kirchner, R. M.; Smith, J. V. *Nature* **1978**, *271*, 512–516.
(20) Zhdanov, S. P.; Feoktistova, N. N.; Kozlova, N. I.; Piryutko, M. M. *Bull. Acad. Sci. USSR, Div. Chem. Sci.* **1985**, *34*, 2467–2472.
(21) Hayhurst, D. T.; Nastro, A.; Aiello, R.; Crea, F.; Giordano, G. *Zeolites* **1988**, *8*, 416–422.
(22) Shen, Z. J.; Zhao, Z.; Peng, H.; Nygren, M. *Nature* **2002**, *417*, 266–269.
(23) Munir, Z. A.; Anselmi-Tamburini, U.; Ohyanagi, M. *J. Mater. Sci.* **2006**, *41*, 763–777.
(24) Nygren, M.; Shen, Z. J. *Solid State Sci.* **2003**, *5*, 125–131.
(25) Vasiliev, P. O.; Shen, Z. J.; Hodgkins, R. P.; Bergstrom, L. *Chem. Mater.* **2006**, *18*, 4933–4938.
(26) Akhtar, F.; Vasiliev, P. O.; Bergstrom, L. *J. Am. Ceram. Soc.* **2009**, *92*, 338–343.
(27) Delhez, R.; Keijser, T. H. D.; Langford, J. L.; Louër, D.; Mittemeijer, E. J.; Sonnefeld, E. J. In *Crystal imperfection broadening and peak shape in the Rietveld method*; Oxford University Press: Oxford, 1993.
(28) Balzar, D.; Audebrand, N.; Daymond, M. R.; Fitch, A.; Hewat, A.; Langford, J. I.; Le Bail, A.; Louer, D.; Masson, O.; McCowan, C. N.; Popa, N. C.; Stephens, P. W.; Toby, B. H. *J. Appl. Crystallogr.* **2004**, *37*, 911–924.
(29) Rodríguez-Carvajal, J. *Commission on Powder Diffraction (IUCr) Newsletter* **2001**, *26*, 12–19.
(30) Verduijn, J. P. Process for producing substantially binder-free zeolite. US patent 5460796, 1997.
(31) Greaves, G. N.; Meneau, F.; Kargl, F.; Ward, D.; Holliman, P.; Albergamo, F. *J. Phys.: Condens. Matter* **2007**, 19.
(32) Greaves, G. N.; Meneau, F.; Majerus, O.; Jones, D. G.; Taylor, J. *Science* **2005**, *308*, 1299–1302.
(33) Peral, I.; Iniguez, J. *Phys. Rev. Lett.* **2006**, 97.
(34) Olson, D. H.; Haag, W. O., Structure-selectivity relationship in xylene isomerisation and selective toluene disproportionation In *ACS Symposium Series*, Whyte, T. E., Jr.; Betta, R. A. D.; Derouane, E. G.; Baker, R. T. K., Eds.; American Chemical Society: Washington, DC, 1984; Vol. 248.
(35) Hedlund, J.; Ohrman, O.; Msimang, V.; van Steen, E.; Bohringer, W.; Sibya, S.; Moller, K. *Chem. Eng. Sci.* **2004**, *59*, 2647–2657.

AM900760W